Dynamin 2 Is Required for Phagocytosis in Macrophages

By Elizabeth S. Gold,*‡ David M. Underhill,* Naomi S. Morrissette,* Jian Guo,* Mark A. McNiven,§ and Alan Aderem*

*From the *Department of Immunology and the ‡Division of Cardiology, University of Washington, Seattle, Washington 98195; and the §Department of Biochemistry and Molecular Biology, The Center for Basic Research in Digestive Diseases, Mayo Foundation, Rochester, Minnesota 55905*

Summary

Cells internalize soluble ligands through endocytosis and large particles through actin-based phagocytosis. The dynamin family of GTPases mediates the scission of endocytic vesicles from the plasma membrane. We report here that dynamin 2, a ubiquitously expressed dynamin isoform, has a role in phagocytosis in macrophages. Dynamin 2 is enriched on early phagosomes, and expression of a dominant-negative mutant of dynamin 2 significantly inhibits particle internalization at the stage of membrane extension around the particle. This arrest in phagocytosis resembles that seen with inhibitors of phosphoinositide 3-kinase (PI3K), and inhibition of PI3K prevents the recruitment of dynamin to the site of particle binding. Although expression of mutant dynamin in macrophages inhibited particle internalization, it had no effect on the production of inflammatory mediators elicited by particle binding.

Key words: phagocytosis • macrophages • dynamin • inflammation • phosphoinositide 3-kinase

Macrophages are "professional phagocytes" that play a critical role in innate and acquired immunity due to their unique ability to internalize and degrade pathogens and to couple this to the release of inflammatory mediators. Phagocytosis is initiated by the interaction of specific receptors on the surface of the phagocyte with ligands on the particle. Although all phagocytosis requires actin polymerization, phagocytosis mediated through different receptors uses distinct mechanisms and results in different biological outcomes (1). Thus, macrophage phagocytosis of pathogens initiates inflammation, whereas the phagocytosis of apoptotic cells does not initiate a proinflammatory response (2). The specific molecular regulators of particle internalization and the mechanisms of coupling to the production of inflammatory mediators are largely unknown.

While cells use phagocytosis to internalize large particles, soluble ligands are internalized through receptor-mediated endocytosis, a clathrin-based process. Dynamin 2 is a ubiquitously expressed GTPase that has a critical role in the scission of forming clathrin-coated endocytic vesicles from the plasma membrane (3). Flies with a temperature-sensitive mutation in *shibire*, the *Drosophila* homologue of dynamin, have impaired endocytosis at the synaptic junction that results in their rapid paralysis at the nonpermissive temperature (4, 5). The nerve terminals of these mutant flies are depleted of synaptic vesicles and have an accumulation of partially invaginated coated pits at the cell surface (6). This defect in endocytosis is also found in several other tissues in these flies (7–9).

In mammalian cells, dominant-negative mutant forms of dynamin that are unable to bind GTP inhibit receptor-mediated endocytosis (10–12). When permeabilized nerve termini are treated with the nonhydrolyzable GTP analogue, GTPγS, tubular membrane invaginations coated with helical arrays of dynamin are formed (13). Similarly, dynamin assembles into collar-like rings around the neck of the tubular liposomes, and hydrolysis of GTP by dynamin leads to an active scission of these tubules into discrete vesicles (14–16). The precise mechanism by which dynamin functions in vesicle scission is controversial; some evidence supports dynamin acting as a mechanical force generator (13–15), whereas other data suggest that it acts as a classical GTPase switch that activates a downstream effector (17).

Dynamin 2 is also involved in membrane traffic at the trans-Golgi network (TGN).[1] A neutralizing antibody directed against dynamin 2 inhibits the formation of both clathrin- and non–clathrin-coated vesicles at the TGN in vitro (18). There is also strong evidence that the *Saccharomyces cerevisiae* dynamin homologue, Vps1p, modulates vesicular trafficking from the TGN (19).

Dynamin 2 is targeted to forming endosomes through its interaction with the Src homology (SH) 3 domain of amphiphysin (20–22). Thus, overexpression of the SH3 do-

[1]*Abbreviations used in this paper:* eGFP, enhanced GFP; GFP, green fluorescent protein; LDL, low-density lipoprotein; PI3K, phosphoinositide 3-kinase; RP, resident peritoneal; SH, Src homology; TGN, trans-Golgi network; TRITC, tetramethyl rhodamine isothiocyanate.

 J. Exp. Med. © The Rockefeller University Press • 0022-1007/99/12/1849/08 $5.00
Volume 190, Number 12, December 20, 1999 1849–1856
http://www.jem.org

main of amphiphysin blocks receptor-mediated endocytosis at nerve terminals and in Cos-7 cells (23, 24). We recently cloned amphiphysin from an expression library using an mAb generated against mouse macrophage phagosomes, and have shown that amphiphysin is enriched on phagosomes (our unpublished results). This suggested a possible role for dynamin in phagocytosis. We report here that dynamin 2 localizes to forming phagosomes, and that a mutant form of dynamin 2 inhibits phagocytosis at the stage of membrane extension around the particle, but does not impair particle-mediated stimulation of inflammatory mediators.

Materials and Methods

DNA Expression Vectors. Full-length dynamin 2 (aa isoform) with a single amino acid mutation that changed the lysine at position 44 to an alanine, dyn^{K44A}, was cloned into the pTIGZ2 vector. In this vector, expression of dyn^{K44A} is under the control of a tetracycline-repressible promoter. Removal of tetracycline from the media results in a bicistronic mRNA that concomitantly directs translation of the dominant-negative dynamin protein and green fluorescent protein (GFP). pTIGZ2 consists of pcDNA3.1/Zeo (Invitrogen) in which the CMV promoter was replaced by the tetracycline-regulated promoter from pTetSplice (XhoI-HindIII fragment; GIBCO BRL) followed by a multiple cloning site, the cap-independent translational enhancer region of pCITE (amplified using the 5′ primer, GTGGATCCGTTATTTTCCACCATATT, and the 3′ reverse primer, GGGAGCTCCCATATTATCATCGTGTT; Novagen) and the coding region for enhanced GFP (eGFP) from peGFP-N1 (EcoRI-NotI fragment; Clontech).

V5 epitope–tagged dynamin 2 and dyn^{K44A} were constructed by TA cloning into the pcDNA3.1/V5/HisTOPO vector (Invitrogen).

pNeo/Tak was constructed to direct expression of the tetracycline transactivator under neomycin selection. The plasmid uses a tetracycline-regulated promoter to direct expression of the tetracycline transactivator (both from pTet-Tak; GIBCO BRL). The neomycin resistance marker was from pcDNA3 (Invitrogen), and the remainder of the plasmid was derived from pBluescript SK (Stratagene).

Immunofluorescence Characterization. Murine resident peritoneal (RP) macrophages were isolated and cultured as described previously (1). Synchronized phagosomes were created by centrifuging particles onto the cells at 1,600 rpm and 4°C for 1 min. (Before exposure to $C3b_i$-opsonized particles, cells were treated with 200 nM PMA for 30 min.) After washing with PBS, the cells were incubated in media at 37°C for the times indicated in the Results. The cells were fixed in formalin (10 min, room temperature), permeabilized in 0.25% Triton X-100 in PBS (10 min, room temperature), washed twice in PBS, and incubated with primary antibody (Dyn 2, an affinity-purified anti-dynamin 2 antibody generated as described [25]; MC63, an anti-pan dynamin antibody generated as described [26]; or the anti-V5 antibody [Invitrogen], and anti–human RBC antibody purchased from Jackson ImmunoResearch Labs) for 1 h at room temperature. The coverslips were washed in PBS and incubated with the appropriate secondary antibodies (all FITC- and TxR-conjugated antibodies were from Cappel, Cy5 conjugates from Jackson ImmunoResearch Labs). Actin was stained with rhodamine-phalloidin (Molecular Probes). After a 1-h incubation, the slides were washed in PBS, rinsed briefly in distilled water, and mounted in a polyvinyl alcohol–based mounting medium (Harlow and Lane). All confocal images were obtained on a Zeiss Axiophot microscope equipped with Bio-Rad confocal optics.

IgG-coated RBCs were prepared by incubating fresh human RBCs, diluted in PBS, with anti–human glycophorin IgG (Jackson ImmunoResearch Labs) at room temperature for 60 min. Complement-coated RBCs were prepared by incubating human red cells with anti–human glycophorin IgM (supernatant from the NN3 hybridoma; American Type Culture Collection) at room temperature for 30 min, and the cells were then washed and resuspended in RPMI with 10% C5-depleted human serum (Sigma Chemical Co.), and incubated at 37°C for 1 h. Zymosan (Molecular Probes) was prepared as described previously (27).

Phosphoinositide 3-kinase (PI3K) was inhibited by incubating RP macrophages with 100 nM wortmannin (Sigma Chemical Co.) for 1 h. These cells were incubated with zymosan for 10 min, then prepared and examined as above.

Immunoblotting. Macrophages, either RP or RAW 264.7 cells (American Type Culture Collection), were lysed on ice into lysis buffer (20 mM Tris, pH 7.4, 120 mM NaCl, 10% glycerol, 2 mM EDTA, 1 mM dithiothreitol, and 1% SDS, 0.09 trypsin inhibitor units [TIU] aprotinin, 0.5 mg/ml leupeptin, 1 mM PMSF). Total murine brain homogenate was lysed into brain lysis buffer (10 mM Hepes, 150 mM NaCl, 10 mM benzamidine, 1% Triton X-100 with the same protease inhibitors as above), incubated at 4°C with agitation for 1 h, and insoluble material was removed by centrifugation at 40,000 *g* for 1 h at 4°C. Samples were quantified by the BCA assay (Pierce Chemical Co.), and 20 μg of protein/well was run on a 10% SDS-PAGE acrylamide gel. Proteins were transferred to polyvinylidene difluoride (PVDF) membrane (Millipore) and blocked overnight at 4°C in 10% nonfat dried milk in PBS. Membranes were incubated for 1 h at room temperature with one of the anti-dynamin antibodies (either Dyn 2 [25] or the anti-dynamin 1 rabbit polyclonal antibody DG2, provided by Pietro De Camilli, Yale University School of Medicine, New Haven, CT), washed three times for 15 min each in TBS/Tween and incubated in a 1:10,000 dilution of peroxidase-conjugated secondary antibody (Cappel). After three 15-min washes in TBS/Tween, specific binding was detected using chemiluminescence (Amersham Pharmacia Biotech).

Cell Surface Staining. Cells to be stained for FcγRII and FcγRIII were resuspended into FACS® buffer (PBS, 2% FCS, 0.5 mM azide) while cells to be stained for Mac-1 were resuspended into 2.4G2 supernatant (American Type Culture Collection), then incubated for 15 min on ice. Primary antibody (biotinylated 2.4G2 for FcR staining or biotinylated anti–mouse CD11b antibody, both from PharMingen) was added, and the cells were incubated on ice for 20 min. Cells were washed in FACS® buffer, resuspended in diluted streptavidin-PE (Caltag), and incubated on ice for 15 min. The cells were washed, resuspended in FACS® buffer with 1% paraformaldehyde, and analyzed on a FACScan™ (Becton Dickinson).

Transfections. A tetracycline transactivator–expressing RAW cell line was generated by transfecting RAW 264.7 cells with pNeo/Tak, and stable cell lines were selected using 400 μg/ml G418 (GIBCO BRL). After 10 d of selection, the cells were cloned by limiting dilution, and one cell line (designated RAW-TT10) that demonstrated good tetracycline-regulated expression from a subsequently transfected reporter plasmid was used for all experiments. In the experiments reported here, tetracycline was always absent from the media, resulting in strong activity of the tetracycline-regulated promoter.

RAW-TT10 cells were transiently transfected by electroporation. 10 μg of DNA was added to 5×10^6 RAW-TT10 cells in 250 μl of RPMI (JRH Biosciences) with 10% heat-inactivated

FCS (Hyclone). The cells were electroporated at 280 V, capacitance 960 μF, and immediately washed in 5 ml of RPMI with 10% FCS. The cells were plated and analyzed 18–24 h later by FACS® or confocal microscopy.

Phagocytosis Assay. Tetramethyl rhodamine isothiocyanate (TRITC)-zymosan was purchased from Molecular Probes. TRITC-labeled SRBC "ghosts" were prepared by incubating SRBCs (ICN/Cappel) in hypotonic lysis buffer (1 mM $MgCl_2$, 100 μM EGTA in 0.02× PBS) with TRITC-BSA (Molecular Probes) on ice for 1 h. Isotonicity was restored to the cells with 5× PBS, and the ghosts were resealed at 37°C for 1 h. Unincorporated TRITC-BSA was removed by washing in PBS, and the ghosts were opsonized as described above (anti-SRBC IgG and IgM were purchased from Intercell).

The specified particles were centrifuged onto the transiently transfected RAW-TT10 cells at 1,600 rpm and 4°C for 1 min. (Before exposure to $C3b_i$-opsonized particles, cells were treated with 200 nM PMA for 30 min.) The cells were incubated at 37°C for 10 min. The extracellular particles were removed, ghosts were lysed with a 20-s water wash, and the TRITC-zymosan was digested for 10 min with 100 U/ml lyticase (Sigma Chemical Co.). The cells were resuspended in PBS/EDTA, fixed with 1% formalin, and analyzed by FACS®.

The effect of dynamin 1 on phagocytosis was assessed with three dominant-negative mutants of dynamin 1 expressed in pCMV5: DI ΔPH (deletion of amino acids 541–618), DI K535M, and DI N272 (deletion of amino acids 1–272) (28). Each of these constructs was cotransfected with pSFFV-eGFP (eGFP under the control of the spleen focus–forming virus LTR) into RAW-TT10 cells, and phagocytosis was assayed as described above.

TNF Assay. RAW-TT10 cells were transfected with dyn^{K44A}-pTIGZ2 18 h before the assay. The cells were incubated with the indicated particles at 37°C for 30 min, at which time 5 μM brefeldin A was added to the media. The zymosan particles were endotoxin free as assessed by the limulus amebocyte lysate assay (QCL-1000; BioWhittaker). The cells were incubated for an additional 2.5 h, then collected for staining. The cells were blocked in 2.4G2 hybridoma supernatant (American Type Culture Collection) for 15 min on ice, fixed in 4% paraformaldehyde for 15 min at room temperature, washed, and stained with anti–TNF-α antibody (PharMingen) conjugated to PE in permeabilization buffer (1% FCS, 0.1% [wt/vol] sodium azide, 0.1% [wt/vol] saponin, in PBS, pH 7.4) at room temperature for 30 min, washed, and analyzed on a FACScan™ (with CELLQuest™ software; both from Becton Dickinson).

Video Microscopy. RAW-TT10 cells were transfected with dyn^{K44A}-pTIGZ and plated on 35-mm glass-bottomed microwell dishes (MatTek Corp.). 18 h later, the dish was mounted on a Zeiss Axiophot microscope equipped with a cooled CCD camera (Princeton Instruments) and Metamorph digital imaging software system (Universal Imaging), and differential interference contrast (DIC) images were collected every 30 s.

Scanning Electron Microscopy. 18 h after transfection, cells expressing high levels of the indicated proteins were sorted onto Thermonox coverslips (Nunc) using a FACStar$^{PLUS™}$ (Becton Dickinson). Cells were adhered for 3 h at 37°C, then incubated with IgG-opsonized SRBCs for the indicated amount of time. Cells were fixed in 3% glutaraldehyde in EM buffer (0.1 M cacodylate, 0.1 M sucrose) at room temperature for 1 h, then washed with EM buffer. The cells were postfixed in 1% OsO_4 in 0.1 M cacodylate, 4 mM CaCl, pH 7.3, for 30 min at room temperature. The cells were dehydrated through serial changes in ethanol (35 and 50%) for 5 min each, en bloc stained in 3% uranyl acetate, 70% ethanol for 30 min, and ethanol dehydration was then completed (80, 90, 95, 100, and 100%, each for 5 min). The coverslips were critical point dried, mounted onto scanning stubs, and air dried overnight. Cells were sputter coated with 30 nm gold/palladium and examined on a Jeol JSM-6300F scanning electron microscope.

Results

Dynamin 2 Is Enriched on Early Phagosomes in Macrophages. Dynamin 2 was found to be expressed in murine RP macrophages and the RAW-TT10 macrophage cell line, whereas dynamin 1 was not detected in macrophages (Fig. 1 A). Interestingly, dynamin 2 was recruited to early phagosomes, as demonstrated by staining with two independent antibodies to dynamin as well as by the localization of the epitope-tagged protein (Fig. 1 B). The phagocytosis of different particles is mediated by different receptors. For example, FcRs mediate the uptake of IgG-coated particles, complement receptors (CRs) mediate the uptake of $C3b_i$-opsonized particles, and the mannose receptor (among others) mediates the uptake of zymosan (yeast cell wall particles) (2). Phagocytosis stimulated by these receptors has common features, such as a reliance on the actin cytoskeleton, and distinct features, such as their different requirement for the cytoskeletal proteins vinculin and paxillin (1). Immunofluorescence microscopy of murine RP macrophages using two independent antibodies demonstrated that dynamin 2 was enriched on early phagosomes containing IgG-opsonized RBCs, $C3b_i$-opsonized RBCs, and zymosan (Fig. 1 B, i, iii, vii, and viii). In addition, an epitope-tagged version of the aa isoform of dynamin 2 transiently expressed in RAW-TT10 macrophages also localized to phagosomes, demonstrating that this macrophage-expressed isoform contains the domain responsible for targeting to phagosomes (Fig. 1 B, iv and v). The kinetics of association of dynamin 2 with phagosomes precisely mirrored that of F-actin: both were recruited to the forming phagocytic cup and the early phagosome (Fig. 1 B, v and vi), and both were concomitantly lost from the phagosome after particle internalization (data not shown).

Dynamin 2 Is Critical for Macrophage Phagocytosis. To examine the role of dynamin 2 in phagocytosis, RAW-TT10 macrophages were transfected with a dominant-negative mutant form of the aa isoform of dynamin 2, dyn^{K44A}, which is unable to bind GTP (11). The mutant dynamin 2 gene was expressed in a bicistronic vector with GFP (pTIGZ2 vector), allowing transiently transfected cells to be identified by their green fluorescence. Phagocytosis of either TRITC-labeled zymosan, IgG-opsonized RBCs, or $C3b_i$-opsonized RBCs was assessed as a function of the level of expression of the GFP/dominant-negative protein by two-color FACS® (Fig. 2). In all cases, dyn^{K44A} inhibited phagocytosis in a dose-dependent manner (Fig. 2 A); a typical FACS® profile is shown in Fig. 2 B. Dyn^{K44A} inhibited FcR-mediated phagocytosis by 85%, CR-mediated phagocytosis by 63%, and zymosan phagocytosis by 65% (Fig. 2 C). As expected, dyn^{K44A} also inhibited receptor-medi-

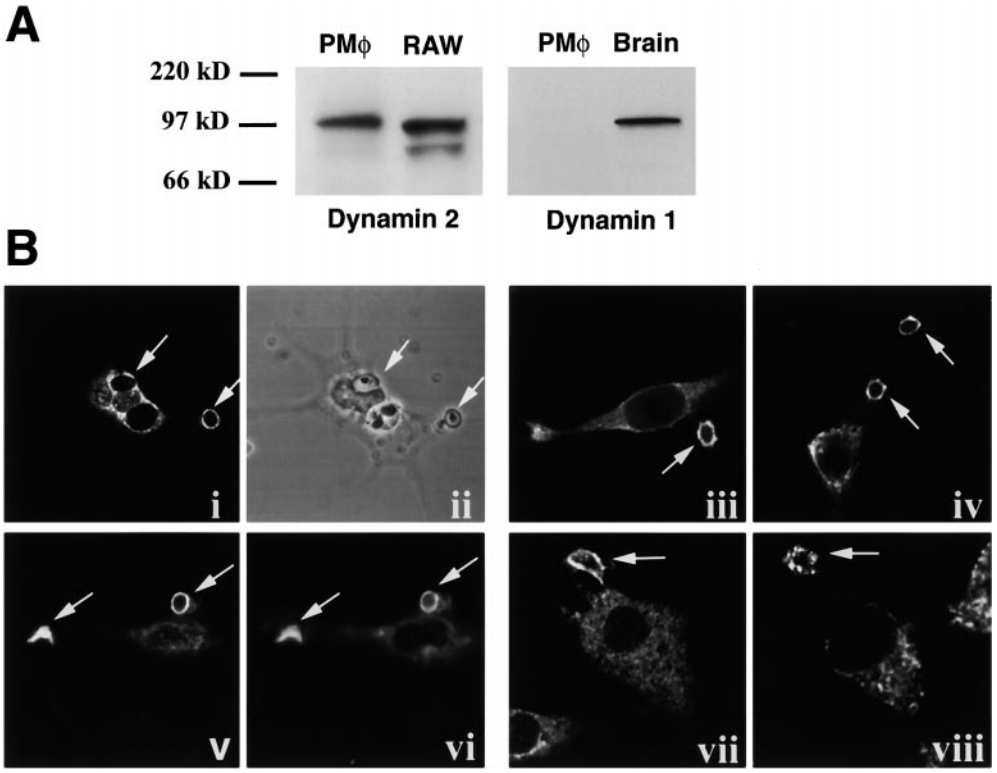

Figure 1. Dynamin 2 is enriched on murine macrophage phagosomes. (A) 20 μg of total protein extract from RP macrophages (PMϕ), RAW-TT10 macrophages, or brain was separated on a 10% SDS-PAGE gel, transferred to polyvinylidene difluoride membrane, and probed with an anti-dynamin 2 (Dyn 2), or an anti-dynamin 1 (DG2) antibody as indicated. A protein of the expected 100-kD size was detected in macrophages by the anti-dynamin 2 antibody but was not detected by the anti-dynamin 1 antibody. (B) Synchronized phagosomes containing either zymosan particles (i–vi), complement-opsonized RBCs (vii), or IgG-opsonized RBCs (viii) were created in RP macrophages (i, ii, iii, vii, viii) or in transiently transfected RAW-TT10 cell expressing V5 epitope–tagged dynamin 2 (iv–vi). 5 min after particle binding, cells were fixed and prepared for immunofluorescence. Dynamin 2 was detected with the anti-dynamin 2 antibody Dyn 2 (i, vii, and viii) or the pan anti-dynamin antibody MC63 (iii); V5 epitope–tagged dynamin was detected with anti-V5 antibody (iv and v); actin was stained with rhodamine-phalloidin (vi); and zymosan was visualized directly (ii). Dynamin enrichment on phagocytic cups and phagosomes (v) colocalized with F-actin (vi).

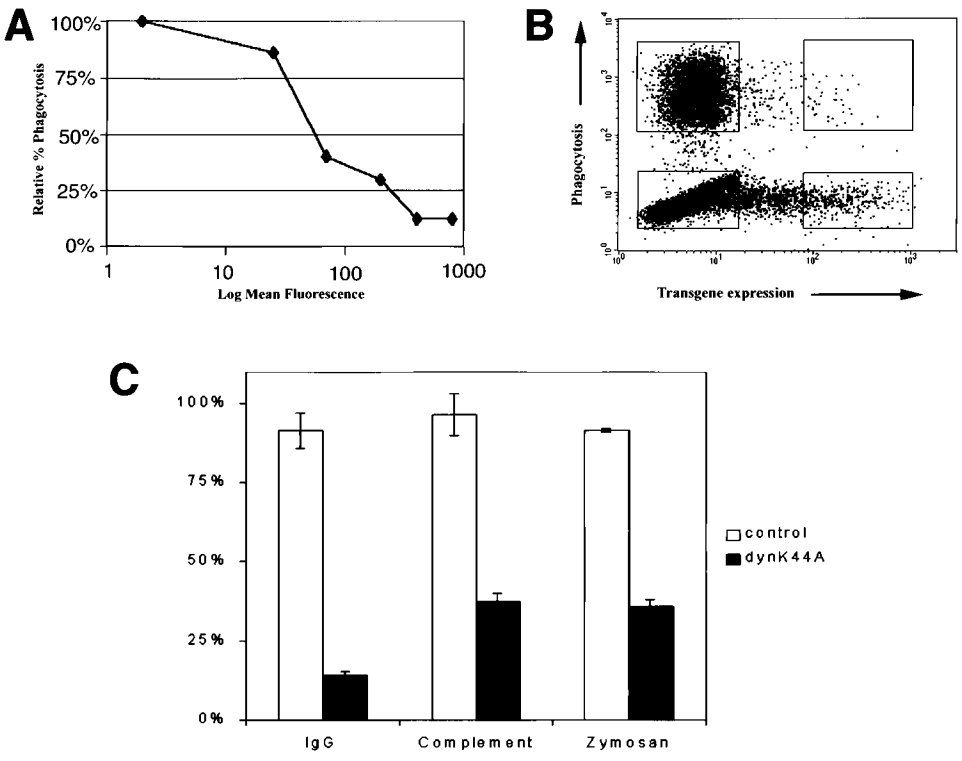

Figure 2. Dyn^{K44A} inhibits macrophage phagocytosis. Transiently transfected RAW-TT10 macrophages internalized the indicated particles for 10 min. Uninternalized particles were removed, and the cells were analyzed by flow cytometry. (A) Dyn^{K44A} inhibited phagocytosis in a dose-dependent manner. Dyn^{K44A} expression, as determined by GFP fluorescence, is plotted on a logarithmic scale on the x-axis. Phagocytosis, expressed as the percentage of cells internalizing particles relative to the percentage of nonexpressing control cells internalizing particles is plotted on the y-axis. The SEM from four independent experiments is shown, but the error bars do not extend beyond the symbols. (B) A typical experiment is shown. RAW-TT10 cells transfected with dyn^{K44A}-pTIGZ2 were incubated with TRITC-zymosan and analyzed. The level of transgene expression is expressed on the x-axis (GFP fluorescence), and the phagocytosis of labeled particles is shown on the y-axis (TRITC fluorescence). (C) RAW-TT10 cells were transiently transfected with either pTIGZ2 vector alone (control) or dyn^{K44A}-pTIGZ2, and phagocytosis of TRITC-loaded IgG-opsonized SRBCs, TRITC-loaded complement-opsonized SRBCs, or TRITC-zymosan was assessed. Phagocytosis is expressed as the percentage of transfected cells internalizing particles relative to the percentage of untransfected cells internalizing particles. Control and dyn^{K44A} cells expressing the same level of GFP were compared. The data shown represent a minimum of three independent experiments, and error bars reflect SEM.

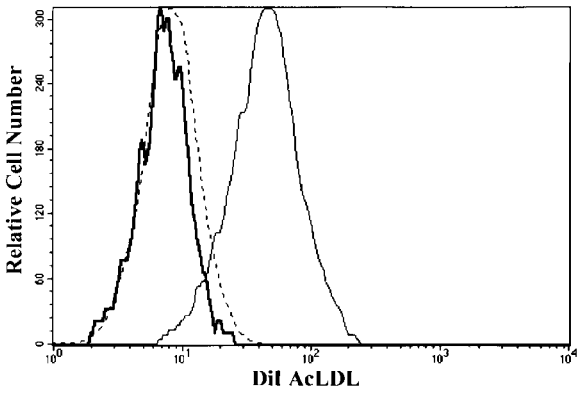

Figure 3. Dynamin 2 blocks receptor-mediated endocytosis in macrophages. RAW-TT10 cells, transfected with the TIGZ control vector (thin solid line) or the dyn^{K44A} vector (thick solid line), were incubated with 20 μg/ml of DiI-labeled acetylated LDL (DiI AcLDL) for 30 min at 37°C. As a control, untransfected cells were incubated with the same concentration of DiI AcLDL at 4°C (dashed line). Cells were collected and analyzed by flow cytometry. The amount of intracellular DiI AcLDL is indicated on the x-axis in log fluorescence units. The histograms were generated by gating on the highly expressing transfected cells (see Fig. 2 B for sample gates). The gates used in this experiment were the same as those used to assay phagocytosis.

ated endocytosis as determined by the uptake of DiI-labeled acetylated low-density lipoprotein (LDL) in macrophages (Fig. 3).

V5 epitope–tagged dyn^{K44A} colocalized with actin on nascent phagocytic cups, demonstrating that the mutant is also recruited to the site of particle-induced signaling and establishing that it is correctly localized to inhibit the function of dynamin on phagosomes (Fig. 4). This construct also inhibited phagocytosis (data not shown), and its effects were indistinguishable from those seen with untagged dyn^{K44A}. These effects were specific for dynamin 2, since dominant-negative mutants of dynamin 1 did not inhibit phagocytosis or receptor-mediated endocytosis in macrophages (data not shown).

The defect in phagocytosis was not due to an effect of dyn^{K44A} on the level of phagocytic receptors, since transfected cells expressed normal cell surface levels of FcRs (CD16 and CD32) and CRs (Mac-1) (data not shown), and particle binding was unimpaired (Table I; and see Figs. 4 and 5). Cell viability and other actin-based processes were unaffected by the expression of dyn^{K44A} as demonstrated by the observations that RAW-TT10 cells expressing dyn^{K44A} were able to migrate, polarize, extend and retract ruffles, and spread in response to phorbol esters (data not shown). Further, engagement of phagocytic receptors stimulated actin polymerization at the site of particle binding (Fig. 4). In addition, mutant dynamin had no effect on particle-induced TNF-α production (see Fig. 7, below), demonstrating that one arm (internalization) of a bifurcating signaling pathway was selectively inhibited.

Dynamin 2 Is Required for Membrane Extension around the Forming Phagosome. Our initial hypothesis was that dynamin would serve a similar role in phagocytosis as it serves in endocytosis and therefore would be required only for scission of the nascent phagosome from the plasma membrane. However, examination of dyn^{K44A}-expressing RAW-TT10 cells attempting to internalize particles revealed that dynamin was exerting a role earlier in the process. Cells expressing dyn^{K44A} were able to bind particles, and phalloidin staining demonstrated that this was accompanied by localized actin polymerization; however, actin extended only partially around the particles (Fig. 4). To determine the stage at which phagocytosis was arrested, dyn^{K44A}-expressing RAW-TT10 cells were studied by scanning electron microscopy. 10 min after contacting IgG-coated SRBCs, control cells (expressing pTIGZ2 alone) were identified at many different stages of particle internalization (Fig. 5 A), while very few of the dyn^{K44A}-expressing cells extended membrane more than halfway around the SRBCs (Fig. 5 B). This indicated that mutant dynamin arrested particle internalization at an intermediate stage. Indeed, after unbound SRBCs were washed away and phagocytosis was allowed to proceed for an additional 50 min at 37°C, the pTIGZ2 control cells had internalized >90% of the particles (Fig. 5 C, and Table I). In contrast, <30% of the particles associated with the dyn^{K44A}-expressing cells were internalized (Fig. 5 D, and Table I).

PI3K is a key regulator of macrophage phagocytosis (29,

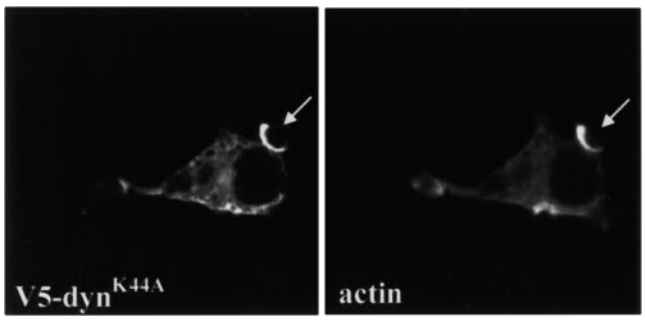

Figure 4. Dyn^{K44A} colocalized with F-actin on phagocytic cups. RAW-TT10 cells transfected with V5 epitope–tagged dyn^{K44A} were incubated with zymosan for 10 min, fixed, and stained with the anti-V5 antibody. Actin was visualized with rhodamine-phalloidin. Arrows indicate where tagged dyn^{K44A} colocalized with actin on partially formed phagocytic cups.

Table I. *Bound, Incompletely Internalized Particles*

	Bound particles	
	10 min	1 h
Control	450 ± 37	35 ± 10
Dyn^{K44A}	480 ± 53	300 ± 28

Data represent number of bound, incompletely internalized IgG SRBCs per 100 macrophages examined by scanning electron microscopy. Error is SEM from three samples. Examination of parallel samples by fluorescence confirmed that after 1 h, >90% of the particles on the control cells were internalized, whereas <30% of the particles associated with the dyn^{K44A}-expressing cells were internalized.

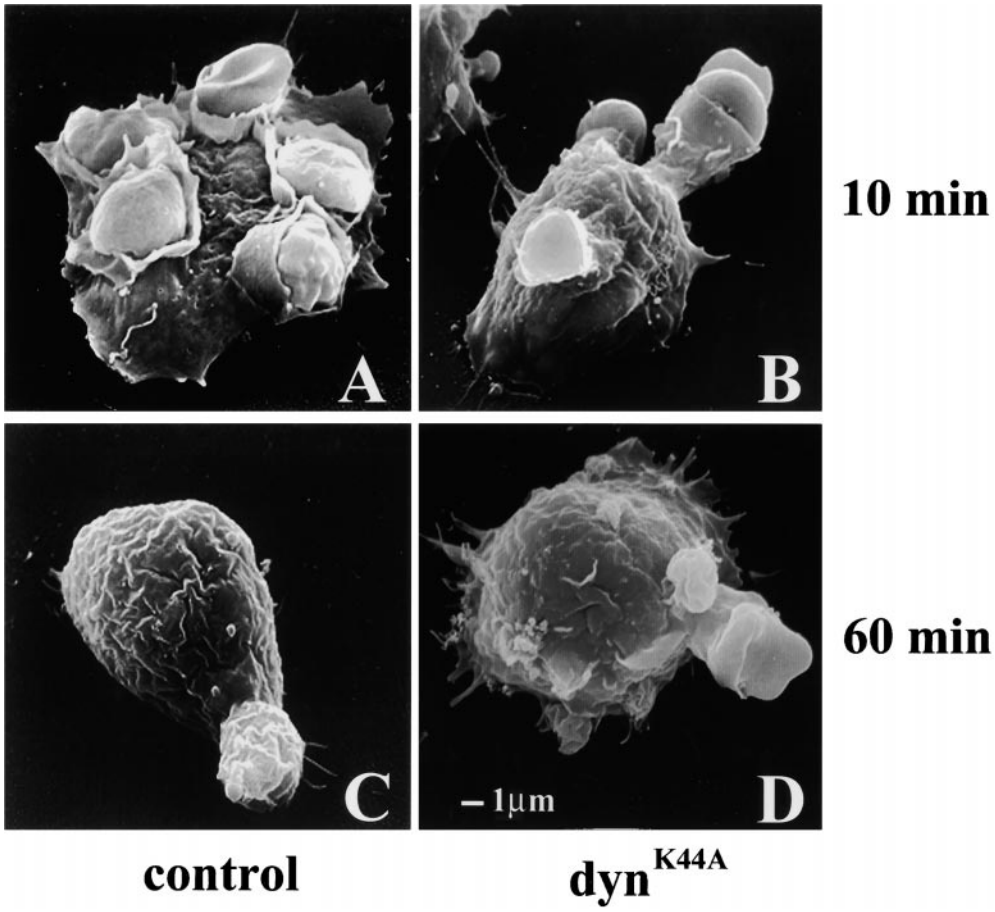

Figure 5. Dyn^{K44A} inhibits membrane extension around the forming phagosome. Transiently transfected cells were sorted by FACS®, and cells expressing the highest levels of GFP were studied by scanning electron microscopy. Sorted cells were incubated with IgG-coated SRBCs for 10 min (A and B) or for 1 h (C and D). After a 10-min internalization, control pTIGZ2–transfected cells demonstrated various stages of particle internalization (A), and after 1 h, >90% of the particles were internalized (C). By contrast, cells expressing dyn^{K44A} could only extend membrane partially around the bound particles at both time points (B and D). The size bar shown in D applies to A–D.

30). Inhibition of PI3K causes incomplete phagosome closure (29, 30), a very similar phenotype to that observed in cells expressing mutant dynamin. Inhibition of PI3K with wortmannin prevented the recruitment of dynamin 2 to the site of particle binding and actin polymerization (Fig. 6, A and B). Thus, it is possible that PI3K might act upstream of dynamin in phagocytosis.

Dynamin 2 Selectively Uncouples Particle Internalization from Particle-induced Cytokine Production. Macrophage phagocytosis of IgG-coated particles and zymosan results in several signaling events, including the production of inflammatory mediators such as TNF-α (2). Cells expressing dyn^{K44A} generated normal amounts of TNF-α upon interaction with particles (Fig. 7); thus, mutant dynamin uncoupled particle internalization from particle-dependent cytokine production.

Discussion

In this study, we have demonstrated that dynamin 2 is essential to the formation of macrophage phagosomes, and that it functions at the stage of membrane extension around the particle. This role for dynamin is conserved in all of the

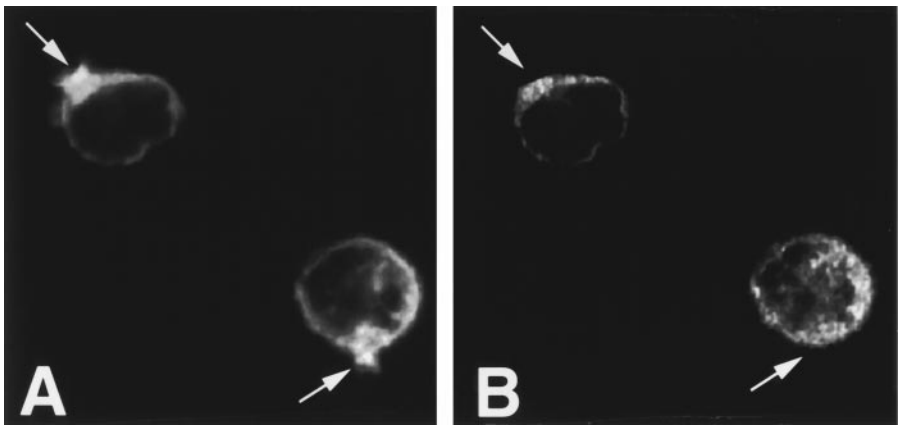

Figure 6. Dynamin is not recruited to the site of particle binding in macrophages treated with the PI3K inhibitor, wortmannin. Murine RP macrophages were treated with wortmannin for 1 h and incubated with zymosan for 10 min. Arrows indicate the site of zymosan binding. Actin polymerized under the bound particles (A), but dynamin was not enriched in the actin pedestals (B).

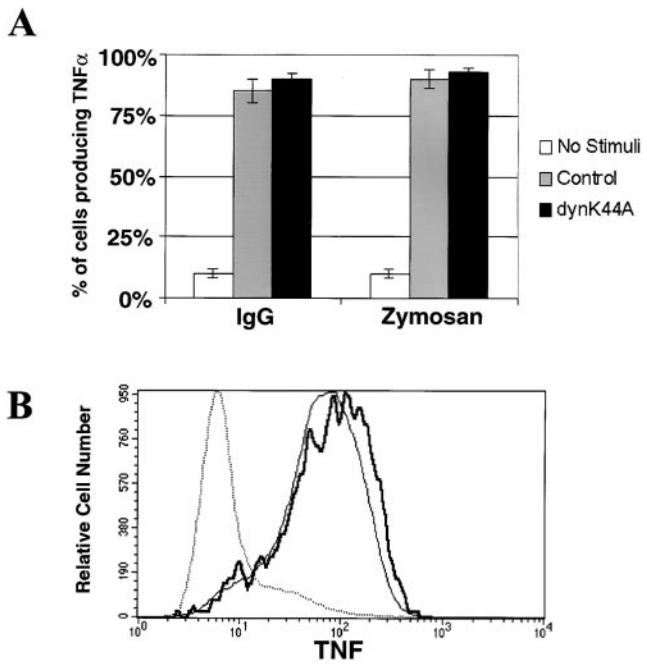

Figure 7. Dyn^{K44A} does not inhibit particle-induced inflammatory signaling. TNF-α production induced by IgG-opsonized particles or by zymosan was analyzed by intracellular cytokine staining in RAW-TT10 cells transiently transfected with either control vector or dyn^{K44A}. Complement-opsonized particles do not stimulate TNF-α production in macrophages and therefore were not analyzed. (A) TNF-α production is expressed as the percentage of transfected cells producing the cytokine. (B) The amount of intracellular TNF-α produced per cell is expressed on the x-axis as log fluorescence units. Unstimulated cells are represented by the dotted line; nonexpressing control cells exposed to zymosan are shown by the bold solid line; and cells expressing high levels of dyn^{K44A} that were stimulated with zymosan are represented by the thin solid line.

phagocytic receptor systems examined. Dominant-negative mutant dynamin did not impinge on the cell's capacity to polymerize actin beneath the particle, or to produce inflammatory mediators such as TNF-α in response to particle binding.

The phagocytic defect induced by dyn^{K44A} resembles that seen when PI3K is inhibited in macrophages (29, 30). This is of interest, since dynamin interacts with the p85 regulatory subunit of PI3K and this interaction stimulates dynamin's GTPase activity (31). We report here that inhibition of PI3K prevents the recruitment of dynamin 2 to the site of particle binding, suggesting that the activation of PI3K is upstream of dynamin in mediating phagocytosis. PI3K supports phagocytosis in macrophages, in part, by facilitating the insertion of membrane into forming phagosomes (30). The scanning electron micrographs shown here suggest that membrane extension may also be the stage of arrest in the cells expressing dyn^{K44A}. Membrane extension is known to require the fusion of vesicles with the plasma membrane (30, 32–35); thus, it is tempting to speculate that dynamin's role in phagocytosis is related to its capacity to recruit membrane to nascent phagosomes. In support of this, the yeast homologue of dynamin, Vps1p, is required for bidirectional trafficking between endosomes and the vacuole (19).

Although our data suggest a role for dynamin 2 in extending membrane around the nascent phagosome, it does not rule out other mechanisms for dynamin's effect on phagocytosis. For example, dynamin might have a direct effect on actin during phagosome formation, since it has been demonstrated to interact with profilin, an actin-binding protein (36). It remains possible that dynamin is also involved in the scission of the neck behind the phagosome, similar to its known role in endocytosis. However, we have not observed any enrichment of dynamin at the scission site of the phagosome.

The phagocytosis of pathogens by macrophages is tightly coupled to the elaboration of inflammatory cytokines that, in turn, orchestrate an appropriate immune response. It has long been known that particle binding by macrophages induces actin-mediated internalization and inflammatory mediator production through a bifurcating signaling cascade (37, 38). Dynamin clearly regulates the particle internalization limb of this pathway while it has no role in the production of inflammatory cytokines.

We thank Dr. Pietro De Camilli for providing the antibody to dynamin 1, Dr. Joseph Albanesi (University of Texas Southwestern Medical Center, Dallas, TX) for providing expression vectors containing the dominant-negative dynamin 1 mutations, Jessica Hamerman and Adrian Ozinsky for critical review of the manuscript, Stephanie Lara for help with scanning electron microscopy, and Kathy Allen for operating the FACStar™.

This work was supported by grant AI-R37-25032 and AI-R01-32972 from the National Institutes of Health. E.S. Gold was supported by grants from the American Heart Association and the Cardiofellows Foundation, and D.M. Underhill is an Irvington Institute postdoctoral fellow.

Address correspondence to Alan Aderem, Department of Immunology, Box 357650, 1959 N.E. Pacific Ave., Seattle, WA 98195. Phone: 206-616-5045; Fax: 206-616-7237; E-mail: aaderem@u.washington.edu

Submitted: 24 August 1999 Revised: 6 October 1999 Accepted: 7 October 1999

References

1. Allen, L.-A., and A. Aderem. 1996. Molecular definition of distinct cytoskeletal structures involved in complement- and Fc receptor–mediated phagocytosis in macrophages. *J. Exp. Med.* 184:627–637.
2. Aderem, A., and D.M. Underhill. 1999. Mechanisms of phagocytosis in macrophages. *Annu. Rev. Immunol.* 17:593–623.

3. Schmid, S.L., M.A. McNiven, and P. De Camilli. 1998. Dynamin and its partners: a progress report. *Curr. Opin. Cell Biol*. 10:504–512.
4. VanderBliek, A.M., and E.M. Meyerowitz. 1991. Dynamin-like protein encoded by the *Drosophila shibire* gene associated with vesicular traffic. *Nature*. 351:411–414.
5. Poodry, C.A., L. Hall, and D.T. Suzuki. 1973. Developmental properties of *shibire*^{ts1}: a pleiotropic mutation affecting larval and adult locomotion and development. *Dev. Biol*. 32:373–386.
6. Kosaka, T., and K. Ikeda. 1983. Possible temperature-dependent blockage of synaptic vesicle recycling induced by a single gene mutation in *Drosophila*. *J. Neurobiol*. 14:207–225.
7. Kessell, I., B.D. Holst, and T.F. Roth. 1989. Membrane intermediates in endocytosis are labile, as shown in a temperature-sensitive mutant. *Proc. Natl. Acad. Sci. USA*. 86:4968–4972.
8. Koenig, J.H., and K. Ikeda. 1990. Transformational process of the endosomal compartment in nephrocytes of *Drosophila melanogaster*. *Cell Tissue Res*. 262:233–244.
9. Kosaka, T., and K. Ikeda. 1983. Reversible blockage of membrane retrieval and endocytosis in the garland cell of the temperature-sensitive mutant of *Drosophila melanogaster*, *shibire*^{ts1}. *J. Cell Biol*. 97:499–507.
10. Damke, H., T. Baba, D.E. Warnock, and S.L. Schmid. 1994. Induction of mutant dynamin specifically blocks endocytic coated vesicle formation. *J. Cell Biol*. 127:915–934.
11. VanderBliek, A.M., T.E. Redelmeier, H. Damke, E.J. Tisdale, E.M. Meyerowitz, and S.L. Schmid. 1993. Mutations in human dynamin block an intermediate stage in coated vesicle formation. *J. Cell Biol*. 122:553–563.
12. Herskovits, J.S., C.C. Burgess, R.A. Obar, and R.B. Vallee. 1993. Effects of mutant rat dynamin on endocytosis. *J. Cell Biol*. 122:565–578.
13. Takei, K., P.S. McPherson, S.L. Schmid, and P. De Camilli. 1995. Tubular membrane invaginations coated by dynamin rings are induced by GTP-γS in nerve terminals. *Nature*. 374: 186–190.
14. Hinshaw, J.E., and S.L. Schmid. 1995. Dynamin self-assembles into rings suggesting a mechanism for coated vesicle budding. *Nature*. 374:190–192.
15. Sweitzer, S.M., and J.E. Hinshaw. 1998. Dynamin undergoes a GTP-dependent conformational change causing vesiculation. *Cell*. 93:1021–1029.
16. McNiven, M.A. 1998. Dynamin: a molecular motor with pinchase action. *Cell*. 94:151–154.
17. Sever, S., A.B. Muhlberg, and S.L. Schmid. 1999. Impairment of dynamin's GAP domain stimulates receptor-mediated endocytosis. *Nature*. 398:481–486.
18. Jones, S.M., K.E. Howell, J.R. Henley, H. Cao, and M.A. McNiven. 1998. Role of dynamin in the formation of transport vesicles from the trans-Golgi network. *Science*. 279: 573–577.
19. Vater, C.A., C.K. Raymond, K. Ekena, I. Howald-Stevenson, and T.H. Stevens. 1992. The VPS1 protein, a homolog of dynamin required for vacuolar protein sorting in *Saccharomyces cerevisiae*, is a GTPase with two functionally separable domains. *J. Cell Biol*. 119:773–786.
20. David, C., P.S. McPherson, O. Mundigl, and P. DeCamilli. 1996. A role of amphiphysin in synaptic vesicle endocytosis suggested by its binding to dynamin in nerve terminals. *Proc. Natl. Acad. Sci. USA*. 93:331–335.
21. McMahon, H.T., P. Wigge, and C. Smith. 1997. Clathrin interacts specifically with amphiphysin and is displaced by dynamin. *FEBS Lett*. 413:319–322.
22. Volchuk, A., S. Narine, L.J. Foster, D. Grabs, P. De Camilli, and A. Klip. 1998. Pertubation of dynamin II with an amphiphysin SH3 domain increases GLUT4 glucose transporters at the plasma membrane in 3T3-L1 adipocytes. Dynamin II participates in GLUT4 endocytosis. *J. Biol. Chem*. 273:8169–8176.
23. Shupliakov, O., P. Low, D. Grabs, H. Gad, H. Chen, C. David, K. Takei, P. DeCamilli, and L. Brodin. 1997. Synaptic vesicle endocytosis impaired by disruption of dynamin-SH3 domain interactions. *Science*. 276:259–263.
24. Wigge, P., Y. Vallis, and H.T. McMahon. 1997. Inhibition of receptor-mediated endocytosis by the amphiphysin SH3 domain. *Curr. Biol*. 7:554–560.
25. Henley, J.R., E.W. Krueger, B.J. Oswald, and M.A. McNiven. 1998. Dynamin-mediated internalization of caveolae. *J. Cell Biol*. 141:85–99.
26. Henley, J.R., and M.A. McNiven. 1996. Association of a dynamin-like protein with the Golgi apparatus in mammalian cells. *J. Cell Biol*. 133:761–775.
27. Aderem, A.A., W.A. Scott, and Z.A. Cohn. 1984. A selective defect in arachidonic acid release from macrophage membranes in high potassium media. *J. Cell Biol*. 99:1235–1241.
28. Achiriloaie, M., B. Barylko, and J.P. Albanesi. 1999. Essential role of the dynamin pleckstrin homology domain in receptor-mediated endocytosis. *Mol. Cell. Biol*. 19:1410–1415.
29. Araki, N., M.T. Johnson, and J.A. Swanson. 1996. A role for phosphoinositide 3-kinase in the completion of macropinocytosis and phagocytosis by macrophages. *J. Cell Biol*. 135: 1249–1260.
30. Cox, D., C.-C. Tseng, G. Bjekic, and S. Greenberg. 1999. A requirement for phosphatidylinositol 3-kinase in pseudopod extension. *J. Biol. Chem*. 274:1240–1247.
31. Gout, I., R. Dhand, I.D. Hiles, M.J. Fry, G. Panayotou, P. Das, O. Truong, N.F. Totty, J. Hsuan, G.W. Booker, et al. 1993. The GTPase dynamin binds to and is activated by a subset of SH3 domains. *Cell*. 75:25–36.
32. Cannon, G.J., and J.A. Swanson. 1992. The macrophage capacity for phagocytosis. *J. Cell Sci*. 101:907–913.
33. Hackam, D.J., O.D. Rotstein, M.K. Bennett, A. Klip, S. Grinstein, and M.F. Manolson. 1996. Characterization and subcellular localization of target membrane soluble NSF attachment protein receptors (t-SNAREs) in macrophages. Syntaxins 2, 3 and 4 are present on phagosomal membranes. *J. Immunol*. 156:4377–4383.
34. Hackam, D.J., O.D. Rotstein, C. Sjolin, A.D. Schreiber, W.S. Trible, and S. Grinstein. 1998. v-SNARE-dependent secretion is required for phagocytosis. *Proc. Natl. Acad. Sci. USA*. 95:11691–11696.
35. Tapper, H., and S. Grinstein. 1997. Fc receptor-triggered insertion of secretory granules into the plasma membrane of human neutrophils: selective retrieval during phagocytosis. *J. Immunol*. 159:409–418.
36. Witke, W., A.V. Podtelejnikov, A. DiNardo, J.D. Sutherland, C.B. Gurniak, C. Dotti, and M. Mann. 1998. In mouse brain profilin I and profilin II associate with regulators of the endocytic pathway and actin assembly. *EMBO (Eur. Mol. Biol. Organ.) J*. 17:967–976.
37. Aderem, A.A., W.A. Scott, and Z.A. Cohn. 1986. Evidence for sequential signals in the induction of the arachidonic acid cascade in macrophages. *J. Exp. Med*. 163:139–154.
38. Aderem, A.A., W.A. Scott, and Z.A. Cohn. 1984. A selective defect in arachidonic acid release from macrophage membranes in high potassium media. *J. Cell Biol*. 99:1235–1241.